24AM1A-01

Uniform Asymptotic Solutions for Scattered Field by a Coated Conducting Cylinder

Le Hoang Loc [#], Keiji Goto [#1]

[#] *Department of Communication Engineering, National Defense Academy*
Yokosuka, Kanagawa, Japan
[1] keigoto@nda.ac.jp

***Abstract*—We derive two kinds of uniform asymptotic solutions for the high-frequency scattered field when a cylindrical wave is incident on a coated conducting cylinder covered by a thin lossy dielectric material. We show that the extended UTD (uniform geometrical theory of diffraction) solution and the modified UTD solution derived by retaining the higher order term can be applied uniformly in the transition region near the shadow boundary and in the deep shadow region in which the conventional UTD solution produces the substantial errors. The validity of the uniform asymptotic solutions derived here is confirmed by comparing with the exact solution obtained from the eigenfunction expansion.**

I. Introduction

The studies on the high-frequency (HF) scattering by a coated conducting cylinder have been an important rchuwaesearch subject for a variety of applications in the area of the radar cross section, the antennas and propagation, and so on [1]-[6]. However, only a limited number of studies have been reported on the uniform asymptotic solutions for the HF scattered fields by coated conducting cylinders [1]-[5].

In this study, we derive an extended UTD (uniform geometrical theory of diffraction) solution and a modified UTD solution for the HF scattered field applicable in the transition region near the shadow boundary (SB) and in the deep shadow region when a cylindrical wave is incident on a coated conducting cylinder covered by a thin lossy dielectric material [7]-[9]. The validity of the uniform asymptotic solutions derived here is confirmed by comparing with the exact solution obtained from the eigenfunction expansion [1]-[4], [7], [8].

II. Formulation and Integral Representation for the Scattered Field

Figure 1 shows a coated conducting cylinder of radius a covered by a complex dielectric material of thickness $t\ (=a-b)$ and coordinate systems (ρ,ϕ) and (x,y,z). The coated conducting cylinder and the electric line source are placed in parallel and are extended from $-\infty$ to $+\infty$ in the z - direction. In this study, we consider the electric-type scattering problem in which the scattered electric field has only the z - direction component.

The scattered electric field $E_z^d(\mathrm{P})$ arriving at the observation point $\mathrm{P}(\rho,\phi)$ from the counterclockwise direction without encircling the coated cylinder after radiated from the electric line source $\mathrm{Q}(\rho_0,\phi_0)$ can be given as follows [8], [9].

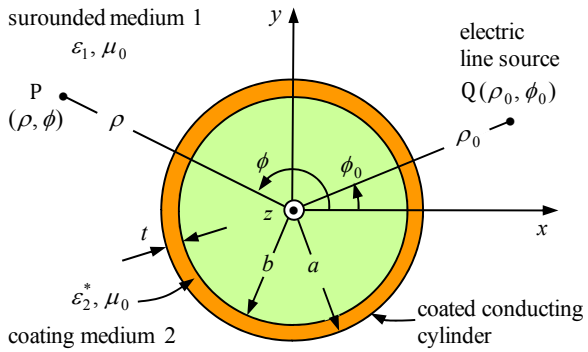

Fig. 1. Coated conducting cylinder covered by a thin lossy dielectric material and coordinate systems (ρ,ϕ) and (x,y,z).

$$E_z^d(\mathrm{P}) = -\frac{i}{8}\int_{-\infty}^{\infty} \frac{H_v^{(2)\prime}(k_1a)+iY_vH_v^{(2)}(k_1a)}{H_v^{(1)\prime}(k_1a)+iY_vH_v^{(1)}(k_1a)} \cdot H_v^{(1)}(k_1\rho_0)H_v^{(1)}(k_1\rho)\exp(iv|(\phi-\phi_0)|)dv \quad (1)$$

$$Y_v = i\frac{Z_1}{Z_2}\cdot\frac{J_v'(k_2^*a)\,Y_v(k_2^*b)-J_v(k_2^*b)\,Y_v'(k_2^*a)}{J_v(k_2^*a)\,Y_v(k_2^*b)-J_v(k_2^*b)\,Y_v(k_2^*a)} \quad (2)$$

$$Z_1=\sqrt{\frac{\mu_0}{\varepsilon_1}},\quad Z_2=\sqrt{\frac{\mu_0}{\varepsilon_2^*}} \quad (3)$$

Here, $H_v^{(1)}(\cdot)$ ($H_v^{(2)}(\cdot)$), $J_v(\cdot)$, and $Y_v(\cdot)$ are respectively the Hankel function of the first (second) kind, the Bessel function, and the Neumann function [10], and the prime ($'$) on these functions denotes the derivative with respect to the argument. $k_1(=\omega(\varepsilon_1\mu_0)^{1/2})$ ($k_2^*=\omega(\varepsilon_2^*\mu_0)^{1/2}$) and Z_1 (Z_2) are the wavenumber and the characteristic impedance in the surrounded homogeneous medium 1 (in the coating medium 2). Notation ε_2^* denotes the complex dielectric constant of the coating material and is defined by $\varepsilon_2^*=\varepsilon_2+i\sigma_2/\omega$ where σ_2 is the conductivity. In (1), the time factor $\exp(-i\omega t)$ is adopted and suppressed in this paper.

The pole singularities v_m $(m=1,\,2,\,3,\cdots)$ determined from the characteristic equation in (1):

$$H_{v_m}^{(1)\prime}(k_1a)+i\,Y_{v_m}H_{v_m}^{(1)}(k_1a)=0\,,\quad m=1,2,3,\cdots \quad (4)$$

and the integration contour in the complex v –plane are shown

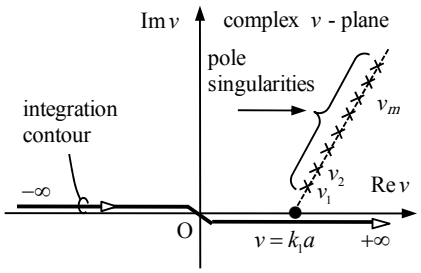

Fig. 2. The integration contour and the pole singularities v_m of the integral in (1) in the complex v –plane.

in Fig. 2

The normalized admittance Y_v in (2) turns indeterminate ($Y_v = 0/0$) when the imaginary part of the variables $k_2^* a$ and $k_2^* b$ of the cylinder functions in (2) is large. In this case, the approximate expression obtained by using these Debye's approximations [5], [10] instead of the cylinder functions under the condition that $k_2^* a$ and $k_2^* b$ become much greater than v is used and is given as follows.

$$Y_v \simeq -i\frac{Z_1}{Z_2}\cdot\frac{\sqrt{(k_2^* a)^2 - v^2}}{k_2^* a}\cot(B_{1,v} - B_{2,v}) \tag{5}$$

$$B_{1,v} = \sqrt{(k_2^* a)^2 - v^2} - v\cos^{-1}\left(\frac{v}{k_2^* a}\right) \tag{6}$$

$$B_{2,v} = \sqrt{(k_2^* b)^2 - v^2} - v\cos^{-1}\left(\frac{v}{k_2^* b}\right). \tag{7}$$

The validity of the approximate expression in (5) is clarified numerically in [8].

III. Uniform Asymptotic Solution for the Scattered Field

Figure 3 shows the direct ray and the reflected ray which arrive at the observation point P_1 located in the deep lit region far away from the SB, the scattered field which arrives at the observation point P_2 in the transition region near the SB, and the surface diffracted ray which arrives at the observation point P_3 in the deep shadow region far away from the SB.

In this section, from the integral in (1), we derive an extended UTD solution and a modified UTD solution applicable uniformly in the transition region near the SB and in the deep shadow region.

A. Extended UTD solution in the Shadow Region

When the observation point is located in the transition region shown in Fig. 3, the main contribution to the integral in (1) arises from the portion of the integration path near $v = k_1 a$ in the complex v -plane. Therefore, one may substitute the Airy function approximations [5] for the Hankel functions $H_v^{(1),(2)}(k_1 a)$ and $H_v^{(1),(2)\prime}(k_1 a)$. The variable is changed from v to τ via $v = k_1 a + M\tau$, $M = (k_1 a/2)^{1/3}$. While, the Hankel functions $H_v^{(1)}(k_1\rho_0)$ and $H_v^{(1)}(k_1\rho)$ are replaced by their second order Debye's approximations [5].

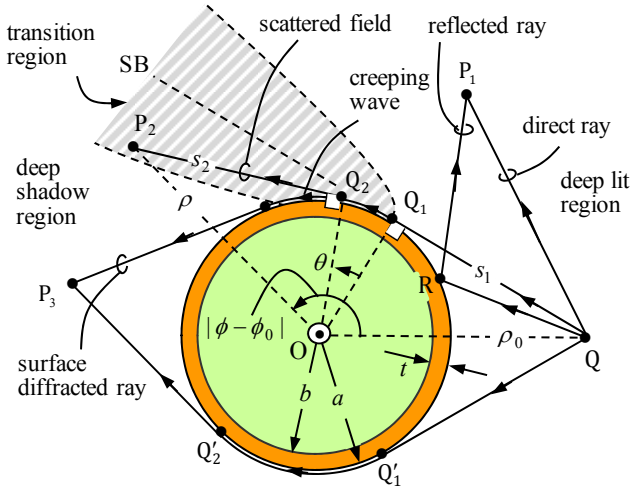

Fig. 3. Direct ray and reflected ray, scattered field, and surface diffracted ray observed at P_1, P_2, and P_3, respectively. Also shown is the transition region near SB.

By performing the straightforward manipulation, one may obtain the following extended UTD solution [8], [9].

$$E_z^d(\mathrm{P}) \sim E_{z,\mathrm{in}}(\mathrm{Q}_1)\, T(\mathrm{Q}_1, \mathrm{Q}_2)\left\{\frac{\exp(ik_1 s_2)}{\sqrt{s_2}}\right\}. \tag{8}$$

Where $E_{z,\mathrm{in}}(\mathrm{Q}_1)$ denotes the incident ray propagating the distance $s_1 (= \overline{\mathrm{QQ}_1} = \sqrt{\rho_0^2 - a^2})$ from the source $\mathrm{Q}(\rho_0, \phi_0)$ to the diffraction point Q_1 and $T(\mathrm{Q}_1, \mathrm{Q}_2)$ denotes the transmission function, which expresses the scattering phenomena occurring along the arc of the coating surface ($\rho = a$) from the point Q_1 to the other diffraction point Q_2 (see Fig. 3). These are defined as follows.

$$E_{z,\mathrm{in}}(\mathrm{Q}_1) = \frac{i}{4}\sqrt{\frac{2}{\pi k_1 s_1}}\exp\,(ik_1 s_1 - i\pi/4) \tag{9}$$

$$T(\mathrm{Q}_1, \mathrm{Q}_2) = -M\sqrt{\frac{2}{k_1}}e^{ik_1\ell}\left[-\frac{F(X)}{2\sqrt{\pi}\xi}e^{-i\frac{\pi}{4}} + P_s^e(\xi, L, q_c(\tau))\right] \tag{10}$$

here the propagation distance $\ell (= a\theta)$ from Q_1 to Q_2 of the creeping wave and the corresponding central angle θ (see Fig. 3), the Fresnel function $F(X)$, and the extended Pekeris function $P_s^e(\xi, L, q_c(\tau))$ are given by

$$\theta = |\phi - \phi_0| - \cos^{-1}\left(\frac{a}{\rho_0}\right) - \cos^{-1}\left(\frac{a}{\rho}\right) \tag{11}$$

$$F(X) = -2iXe^{-iX^2}\int_X^\infty e^{i\tau^2}d\tau\ , X = \sqrt{2k_1 L}\frac{\theta}{2} \tag{12}$$

$$P_s^e(\xi, L, q_c(\tau)) = \frac{\exp(-i\pi/4)}{2\sqrt{\pi}}\int_{i\infty}^0 \frac{w_2'(\tau) - q_c(\tau)w_2(\tau)}{w_1'(\tau) - q_c(\tau)w_1(\tau)}$$

$$\cdot \exp\left[i\xi\tau + i\frac{M^2}{2k_1L}\tau^2\right]d\tau$$

$$+\frac{\exp(-i\pi/4)}{\sqrt{\pi}}\int_0^{\infty}\frac{Ai'(\tau)-q_c(\tau)Ai(\tau)}{w_1'(\tau)-q_c(\tau)w_1(\tau)}$$

$$\cdot \exp\left[i\xi\tau + i\frac{M^2}{2k_1L}\tau^2\right]d\tau \tag{13}$$

$$w_1(\tau) = Ai(\tau) - iBi(\tau),\quad w_2(\tau) = Ai(\tau) + iBi(\tau) \tag{14}$$

$$q_c(\tau) = iMY_v(\tau),\ v = k_1a + M\tau,\ M = \left(\frac{k_1a}{2}\right)^{1/3} \tag{15}$$

$$\xi = M\theta\ ,\quad L = \frac{s_1s_2}{s_1+s_2}. \tag{16}$$

In (8), the term in the brackets { } represents the cylindrical wave propagating the distance $s_2(=\overline{Q_2P_2}=\sqrt{\rho^2-a^2})$ from the diffraction point Q_2 to the observation point P_2.

B. Modified UTD solution in the Shadow Region

The terms in the square brackets [ ] in (10) may be represented by the following extended Pekeris caret function $\hat{P}_s^e(\xi, L, q_c(\tau))$ [8]:

$$\hat{P}_s^e(\xi, L, q_c(\tau)) = \frac{\exp(-i\pi/4)}{\sqrt{\pi}}\int_{C_0}\frac{Ai'(\tau)-q_c(\tau)Ai(\tau)}{w_1'(\tau)-q_c(\tau)w_1(\tau)}$$

$$\cdot \exp\left[i\xi\tau + i\frac{M^2}{2k_1L}\tau^2\right]d\tau \tag{17}$$

where the integration contour C_0 runs along the positive imaginary axis from $+i\infty$ to 0 and then along the positive real axis from 0 to $+\infty$ in the complex v –plane. The higher-order term including τ^2 is retained in the argument of the exponential in the above integral. The extended Pekeis caret function in (17) coincides with the conventional Pekeris caret function [11], [12] when $k_1L \to \infty$ and $|Y_v(\tau)| \to \infty$ (i.e., when $|q_c(\tau)| \to \infty$ in (17)).

When the observation point is located in the shadow region where $\xi(=M\theta)$ satisfies $\xi > 0$, the integral in (17) is evaluated rigorously by applying the Cauchy's residue theorem. Then substituting the residue series solution into (10) and then (10) into (8) and performing the straightforward manipulation yield the following modified UTD solution [8]:

$$E_z^d(\mathrm{P}) \sim E_{z,\mathrm{in}}(\mathrm{Q}_1)\sum_{m=1}^{\infty}\Big\{D_m(\mathrm{Q}_1)A_m(\mathrm{Q}_1)\exp(ik_1\ell - \Omega_m\ell)$$

$$\cdot D_m(\mathrm{Q}_2)A_m(\mathrm{Q}_2)\Big\}\frac{\exp(ik_1s_2)}{\sqrt{s_2}} \tag{18}$$

here the coefficients $D_m(\mathrm{Q}_{1,2})$, $A_m(\mathrm{Q}_{1,2})$, and Ω_m are given by

$$D_m(\mathrm{Q}_{1,2}) = \frac{\sqrt{M}\exp(i\pi/24)}{\sqrt[4]{2\pi k_1}A_i'(-\sigma_m)\sqrt{g_m}} \tag{19}$$

$$g_m = 1 - \frac{\tau_m}{q_c^2(\tau_m)} \tag{20}$$

$$A_m(\mathrm{Q}_{1,2}) = \exp\left[-\frac{M^2\sigma_m^2}{2k_1s_{1,2}}\exp(i\pi/6)\right] \tag{21}$$

$$\Omega_m = \frac{M}{a}\sigma_m\exp(-i\pi/6). \tag{22}$$

Note that the τ^2 term retained in the exponential in (17) corresponds to the terms $A_m(\mathrm{Q}_1)$ and $A_m(\mathrm{Q}_2)$ in (18).

The eigenvalue σ_m and the corresponding τ_m and v_m are obtained from the following characteristic equation

$$w_1'(\tau_m) - q_c(\tau_m)w_1(\tau_m) = 0\ ,\quad m = 1, 2, 3, \cdots \tag{23}$$

$$\tau_m = \sigma_m\exp(i\pi/3)\ ,\quad v_m = k_1a + M\tau_m\ . \tag{24}$$

The residue series in (18) converges when the observation point is located in the region satisfying the condition:

$$\theta > -\frac{a\sigma_{R,m}}{4M^2L},\quad \sigma_{R,m} = \mathrm{Re}[\sigma_m]\ . \tag{25}$$

Where $\mathrm{Re}[\sigma_m]$ denotes the real part of σ_m. In the numerical calculation in Sect. IV, it will be shown that the modified UTD solution in (18) can be applied even in the lit region in the transition region satisfying the inequality in (25). Also shown in Sect. IV is the validity of the modified UTD solution in the deep shadow region where the conventional UTD solution [1] deviates substantially from the exact eigenfunction solution [1]-[4], [6], [7].

IV. Numerical Results and Discussions

In this section, we perform the numerical calculations require to assess the validity of the uniform asymptotic solutions derived in Sect. III.

In Fig. 4(a), the (E-mode type) scattered electric field magnitude curves are calculated by using the asymptotic solutions for the coated conducting cylinder covered by a thin lossy dielectric material. The results correspond to the case when both the source Q and the observation point P are located relatively close to the cylinder surface. The SB is located at $|\phi - \phi_0| = 78.0°$ as shown in the horizontal coordinate.

The exact solution (——) has been calculated from the eigenfunction expansion [1]-[4], [7], [8]. In the lit region $0 \le |\phi - \phi_0| \le$ SB, the geometrical optics (GO) solution (◦◦◦) consisting of the direct ray and the reflected ray is used in the calculation. While in the region $28° \le |\phi - \phi_0| \le 180°$, which includes the deep shadow region far away from the SB, the extended UTD solution (●●●) in (8) associated with (9)-(16), and the modified UTD solution (▫▫▫) in (18) associated with (19)-(22) are applied and are calculated from the superposition of the scattered field in the counter-clockwise and the clockwise direction shown in Fig. 3. It is clarified that the GO solution (◦◦◦), the extended UTD solu-

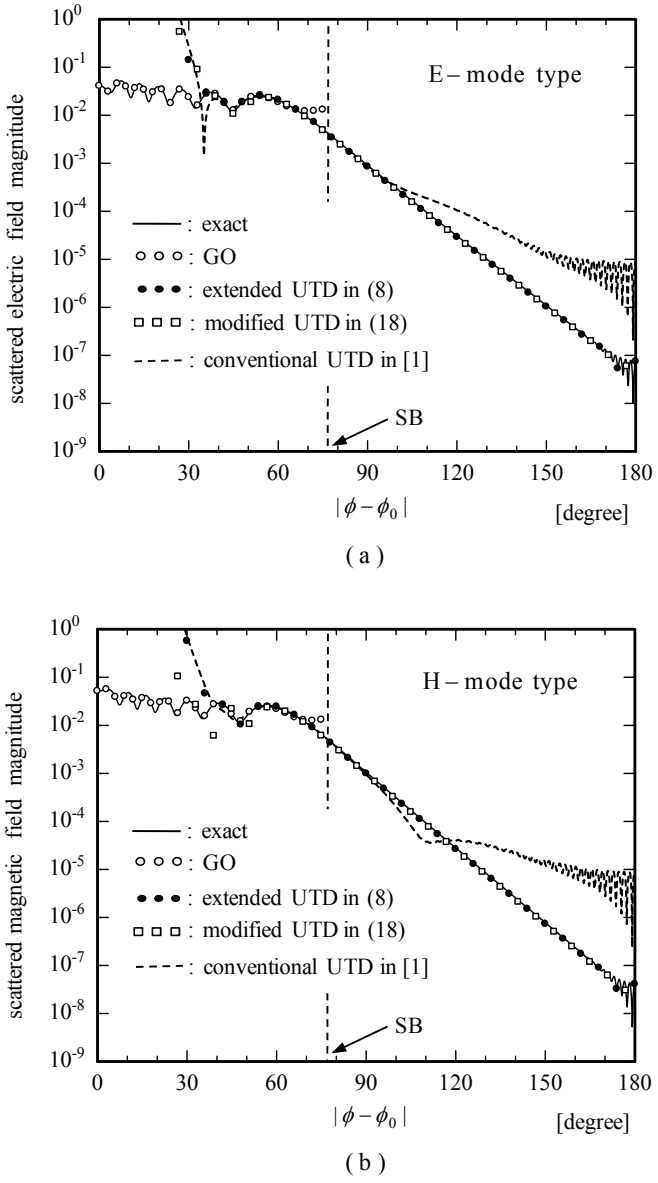

Fig. 4. Scattered fields by the coated conducting cylinder covered by a thin lossy dielectric material calculated from the asymptotic solutions and the exact solution. The numerical parameters used in the calculation: $k_1 a = 100$, $a = 5.0$ m, $t = 0.15\lambda$, $\varepsilon_1 = \varepsilon_0$, $\varepsilon_2 = 5\varepsilon_0$, $\sigma_2 = 0.053$ S/m, source point: $(\rho_0, \phi_0) = (1.2a,\ 0.0°)$ and observation point: $(\rho, \phi) = (1.4a, \phi)$. (a): E-mode type, (b): H-mode type.

tion (●●●), and the modified UTD solution (□□□) agree excellently with the exact solution (——) in the respective regions. Also, shown in Fig. 4(a) is the conventional UTD solution in [1] (– – –). The conventional UTD solution agrees excellently with the exact solution in the lit region. However, in the shadow region, the conventional UTD solution becomes increasingly inaccurate as the observation point moves toward the deep shadow region, i.e., as the value of $|\phi - \phi_0|$ increases in the shadow region.

In Fig. 4(b), we have shown the scattered magnetic field for the H-mode type excited by the magnetic line current. The results for the H-mode type are similar to those for the E–mode type (Fig. 4(a)).

V. Conclusion

We have derived the uniform asymptotic solutions for the scattered field by a coated conducting cylinder covered by a thin lossy dielectric material. The extended UTD solution and the modified UTD solution have been derived by retaining the higher-order term in the exponential in the integral for the scattered field. By comparing with the exact solution calculated from the eigenfunction expansion, we have confirmed the accuracy of the uniform asymptotic solutions proposed here. We have clarified that the uniform asymptotic solutions can be applied even in the deep shadow region where the conventional UTD solution produces the substantial errors.

Acknowledgment

This work was supported in part by the Grant-in-Aid for Scientific Research (C) (24560492) from Japan Society for the Promotion of Science (JSPS).

References

[1] H. T. Kim and N. Wang, "UTD Solution for electromagnetic scattering by a circular cylinder with thin lossy coatings," *IEEE Trans. Antennas Propag*., vol. 37, no. 11, pp. 1463-1472, Nov. 1989.

[2] H. H. Syed and J. L. Volakis, "High-frequency scattering by a smooth coated cylinder simulated with generalized impedance boundary conditions," *Radio Sci*., vol. 26, no. 5, pp. 1305-1314, Sept.-Oct. 1991.

[3] T. B. A. Senior and J. L. Volakis, Eds., *Approximate Boundary Condition in Electromagnetics*, Chap. 7, IEE, London, 1995.

[4] P. E. Hussar, "A uniform GTD treatment of surface diffraction by impedance and coated cylinders," *IEEE Trans. Antennas Propag*., vol. 46, no. 7, pp. 998-1008, July 1998.

[5] T. Ida and T. Ishihara, "Novel high-frequency asymptotic solutions in the transition regions near geometrical boundaries and near caustics for scattering by a dielectric cylinder," *IEICE Trans. Electron*., vol. E87-C, no. 9, pp. 1550-1559, Sept. 2004.

[6] J. Sun and L. W. Li, "Dispersion of waves over a PEC cylinder coated with two-layer lossy dielectric materials," *IEEE Trans. Antennas Propag*., vol. 55, no. 3, pp. 877-881, March 2007.

[7] M. Nakamura, T. Kawano, K. Goto, and T. Ishihara, "A uniform asymptotic analysis of scattered fields by a coated cylinder," *The Papers of Technical Meeting on EMT, IEE Japan*, EMT-07-106, pp. 149-154, Oct. 2007.

[8] K. Goto, L. H. Loc, T. Kawano, and T. Ishihara, "Asymptotic analysis of high-frequency scattered fields by a coated conducting cylinder," *The Papers of Technical Meeting on EMT*, *IEE Japan,* EMT-11-128, pp. 1-6, Nov. 2011.

[9] K. Goto, L. H. Loc, T. Kawano, and T. Ishihara, "Extended UTD solution for scattered fields by a coated conducting cylinder," *Proc. of 2012 IEEE AP-S*, CD-ROM, 358.6, Chicago, USA, July 2012.

[10] M. Abramowitz and I. A. Stegun, Eds., *Handbook of Mathematical Functions*, pp. 358-478, Dover, New York, 1972.

[11] P. H. Pathak, "An asymptotic analysis of the scattering of plane waves by a smooth convex cylinder," *Radio Sci*., vol. 14, no. 3, pp. 419-435, May-June 1979.

[12] G. L. James, Ed., *Geometrical Theory of Diffraction for Electromagnetic Waves*, 3rd ed., chaps 2-6, Peter Peregrinus, London, 1986.